A Multiple-switch Technology for High-power Pulse Discharging

Z. Liu[1], A. J. M. Pemen[1], E. J. M. van Heesch[1], K. Yan[2], G. J. J. Winands[1], D. B. Pawlok[1]
(1 Department of Electrical Engineering, Eindhoven University of Technology, 5600 MB Eindhoven, The Netherlands. E-mail: z.liu@tue.nl
2 Department of Environmental Science, Zhejiang University, Hangzhou 310027, PR China. E-mail: kyan@zju.edu.cn)

Abstract: This article presents our recent research on a new multiple-switch pulsed power technology. With this technique, multiple spark-gap switches can be synchronized automatically, like in Marx generator. However, in contrast to a Marx, Pulsed power can be produced either at a high voltage or with a large current, or it can be used to drive multiple independent loads simultaneously. It is promising for the development of an efficient large pulsed power supply with an increased lifetime. Through use of this technique, an efficient ten-switch prototype system has been successfully developed. Experimental results show that 10 spark-gap switches can be synchronized within about 10 ns. The system has been successfully demonstrated at repetition rates up to 300 pps (Pulses Per Second). Pulses with a rise-time of about 11 ns, a pulse width of about 55 ns, an energy of 9 J-24 J per pulse, a peak power of 300 MW-810 MW, a peak voltage of 40-77 kV, and a peak current of 6 kA-11 kA have been achieved with an energy conversion efficiency of 93%-98%.

Keywords: corona plasma, pulsed power, multiple switching, spark gaps

1 INTRODUCTION

As an enabling technique, pulsed power has been investigated for enormous feasibilities of industrial applications. Up to now, hundreds of possibilities can be anticipated [1-3]. In particular, pulse discharging induced plasma creates highly energetic electrons, ions and reactive radicals. Many researches have been carried out for gas cleaning (VOC, NO_x, SO_2, odor, tar, and etc.). Together with electrostatic precipitator, corona plasma system is expected to simultaneously remove dusts, SO_2, NO_x and heavy metals from exhaust gases. However, successful introduction of pulsed power in large-scale industries depends to a great extent on the availability of highly efficient and reliable cost-effective sources.

Previously introduced single spark-gap switch based nanosecond pulsed power generators [4-6] have been demonstrated both in laboratory and in field trials. They were operated reliably and efficiently (>90%) for the applications with a low power. When scaling these systems up to much higher power levels (e.g. peak power 1 GW, peak current 10 kA-20 kA) [7], the main issue, however, is the electrode erosion of the spark gap switch, which is increased nonlinearly as the switching current increases [8-10]. To solve this problem, a multiple-switch technology was proposed [11]. By interconnecting multiple spark-gap switches via a TLT (Transmission Line Transformer), multiple spark-gap switches can be synchronized automatically like in a Marx generator, and used in parallel equivalently. The heavy switching duty can be shared by multiple switches identically. Since the switching current through each switch is reduced, the lifetime can be expected to improve significantly, compared with a single-switch based system. The fundamental principle of this technology was studied on a two-switch concept and reported previously [12-14]. Through use of this technology, a prototype of an efficient repetitive heavy-duty pulsed power generation has been realized. It adopts ten high-pressure spark gap switches and a 10-stage TLT. With this system, pulses with a rise-time of about 11 ns, a pulse width of about 55 ns, a peak power of 300 MW-810 MW, and a peak current of 6 kA-11 kA have been obtained with an energy conversion efficiency of 93%-98%. In this article, the fundamental principle and the detailed information about the ten-switch prototype will be given.

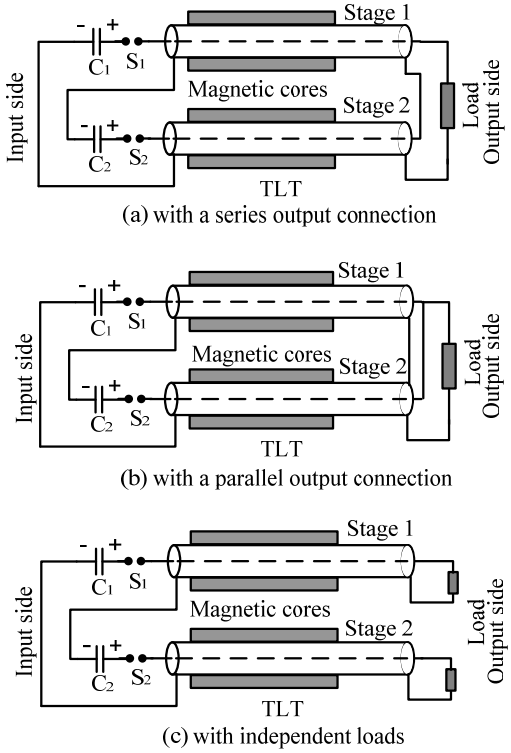

Fig. 1 Schematic diagrams of three circuit topologies with two switches and a 2-stage TLT

2 PRINCIPLE OF THE TECHNOLOGY

Fig. 1 gives examples of the circuit topologies with two spark-gap switches (S_1-S_2) and a two-stage TLT. At the input side of the TLT, two identical capacitors C_1 and C_2 are interconnected to the TLT via two switches. At the output side, the TLT can be put in series for high-voltage generation, as shown in Fig. 1 (a), or in parallel to produce a large current pulse, as shown in Fig. 1 (b), or even can be used to drive independent loads, as shown in Fig. 1 (c). The TLT is made from coaxial cables. Magnetic cores are placed around the cables to increase the secondary mode impedance Z_s, which is defined as the wave impedance between two adjacent stages of the TLT.

To gain insight into the principle, an equivalent circuit for the input side of the TLT is introduced as shown in Fig. 2, under the assumption that the TLT is ideally matched at the output side and the transit time for a pulse propagating along the outsides of the TLT is much longer than the time interval for the synchronization process of the multiple switches. Here each stage is represented by its characteristic impedance Z_0. Following the connections in Fig. 1, it can be seen that both stages (i.e. C_1-S_1-Z_0 and C_2-S_2-Z_0) are connected in series. The secondary mode impedance is represented by Z_s.

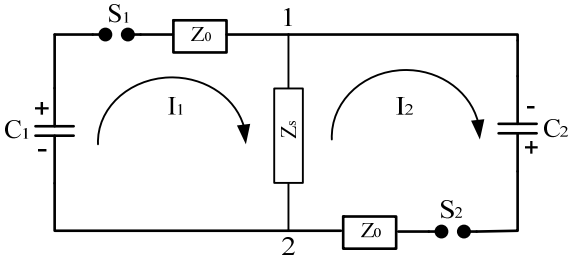

Fig. 2 The equivalent circuit at the input side of the TLT

Initially, two identical capacitors C_1 and C_2 are charged in parallel up to V_0. Whenever one switch (e.g. S_1) is closed and the other one is still open, a voltage V_{12} will be generated over the secondary mode impedance Z_s, which is equal to $[Z_s/(Z_0+Z_s)]\times V_0$. Because the Z_s is designed to be much larger than the characteristic impedance Z_0 of the TLT, the discharging of capacitor C_1 or C_2 is prevented, and the value of V_{12} could be up to V_0. Moreover, because the stray capacitance of the spark gap switch S_1 or S_2 is much smaller than the capacitance of C_1 or C_2, the voltage across the unclosed switch can rise from V_0 up to $V_0+V_{12} \approx 2V_0$. This generated overvoltage will force the second switch to close subsequently.

When all the switches are closed, one can derive the following equations from the equivalent circuit shown in Fig. 2:

$$\begin{cases} I_1(t)\cdot(Z_0+Z_s)-I_2(t)\cdot Z_s = V_0-\dfrac{1}{C_0}\displaystyle\int_0^t I_1(\tau)d\tau \\ I_2(t)\cdot(Z_0+Z_s)-I_1(t)\cdot Z_s = V_0-\dfrac{1}{C_0}\displaystyle\int_0^t I_2(\tau)d\tau \end{cases} \quad (1)$$

In above equations, $I_1(t)$ and $I_2(t)$ are the switching currents through switches S_1 and S_2 respectively, and C_0 is the value of capacitors C_1 and C_2 (C_1 and C_2 are identical). Solving these two equations, one can obtain the following expressions for $I_1(t)$ and $I_2(t)$:

$$I_1(t) = I_2(t) = \frac{V_0}{Z_0}\cdot\exp\left(\frac{-t}{Z_0\cdot C_0}\right) \quad (2)$$

It can be seen that after both switches are closed, the switching currents $I_1(t)$ and $I_2(t)$ are identical and determined by the characteristic impedance Z_0 of the TLT. The voltage V_{12} across Z_s will drop to zero. Now all stages of the TLT are used in parallel equivalently. After a short time delay (transit time of the TLT), an exponential pulse will be generated over the loads at the output side. For all the circuits in Fig. 1, the input impedance Z_{in} of the TLT is the same (i.e. $Z_0/2$). The pulse duration and the peak output power are also the same; the pulse duration is determined by the constant Z_0C_0, and the peak output power is determined by charging voltage V_0 and input impedance Z_{in}, and equals V_0^2/Z_{in}. However, the output voltages and currents are different for different output configurations. For the series output configuration in Fig. 1 (a), the peak output voltage and current are $2V_0$ and V_0/Z_0 respectively. For the parallel output configuration in Fig. 1 (b), the peak output voltage and current are V_0 and $2V_0/Z_0$ respectively. As for the configuration in Fig. 1 (c), the peak output voltage and current on each load are V_0 and V_0/Z_0 respectively.

It is noted that for a practical circuit, although the described equivalent circuit cannot be used to accurately derive the switching behaviors due to the limited secondary mode impedance Z_s and the finite length of the TLT, the model presents the basic principle of the technology.

In principle, the circuit topologies described in Fig. 1 can be extended for any number of switches for high power generation. In addition, the capacitor can be replaced by PFL (Pulse Forming Line) or PFN (Pulse Forming Network) to obtain square pulses. Other kinds of switches, such as solid state switches and magnetic compression switches, can be also used to replace the spark-gap switches.

3 AN EFFICIENT 10-SWITCH PROTOTYPE

Through use of this technology, an efficient heavy-duty repetitive pulsed power generation with a fast rise-time and short pulse width has been developed for nonthermal plasma generation. As shown in Fig. 3, this setup mainly includes 19 charging inductors, 10 high-voltage capacitors, ten spark-gap switches, a ten-stage TLT with one single cable per stage. The ten switches are high-pressure spark gap switches. One of them is a triggered switch [15], while the others are self-breakdown switches. The TLT is made from coaxial cable (RG218) and each stage is 2 m long. Magnetic cores are placed around the coaxial cables for the purpose of synchronization. At the output side of the TLT, all the stages are connected in parallel, thus the output impedance is very low (5 Ω) and a large output current is obtained through multiplying the currents in all the stages.

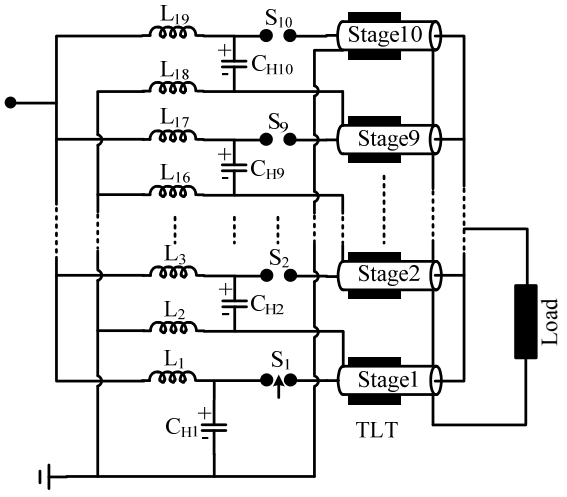

Fig. 3 The electrical circuit of the ten-switch prototype

3.1 Charging Inductors

The nineteen inductors L_1-L_{19}, shown in Fig. 3, are used to charge the high-voltage capacitors in parallel during the charging process. While during the synchronization process of the ten switches, they also provide high impedance to prevent the discharging of the high-voltage capacitors. To ensure proper synchronization, the value L of the inductors must be:

$$L >> \frac{Z_s \cdot \Delta T_s}{2} \tag{3}$$

where ΔT_s is the time interval for the synchronization of all switches. For instance, when Z_s=2 kΩ and ΔT_s=30 ns, the inductance should be much larger than 30 μH. Within the present setup, air-core inductors were used. The inductance value of each inductor is 605 μH.

3.2 Spark Gap Switches

High-pressure spark-gap switches (S_1-S_{10}) were used for the present system. Switch S_1 is constructed as a triggered spark gap switch, while the other switches S_2-S_{10} are self-breakdown switches. The electrodes of each switch are made of brass, and the diameter of each electrode is 20 mm. They were designed to have the same breakdown voltage. For the self-breakdown switches, the gap distance is 4 mm. For the triggered switch, the distances of the trigger gap and the gap between the trigger electrode and the cathode are 1 mm and 2.8 mm respectively.

3.3 The TLT

The TLT plays an important role in the synchronization of the multiple switches and in the transfer of the energy from the capacitors to the load [12]. To ensure the synchronization and to prevent the discharging of the capacitors during the synchronization, the secondary mode impedance Z_s of the TLT must be much larger than the characteristic impedance Z_0 of the coaxial lines, namely:

$$Z_s >> Z_0 \tag{4}$$

To avoid reflections of the high-voltage pulse between the outer conductors of the TLT, the transit time between the outer conductors of the TLT should be longer than $\Delta T_s/2$. Therefore, the length l of the coaxial cables covered by magnetic cores needs to obey:

$$\frac{l}{\upsilon_s} \geq \frac{1}{2}\Delta T_s \tag{5}$$

In the above equation, υ_s is the wave velocity between the outer conductors of the TLT

During the synchronization process of multiple switches, the overvoltage induced by the closing of the first switch is shared by the rest switches that are not closed yet. When a large number of switches are used, the overvoltage may be too small to close the second switch. This may cause the failure of the synchronization of multiple switches. Since the value of the overvoltage across each switch is proportional to the corresponding secondary mode impedance [16], the different secondary mode impedances of the TLT can be used. Thus the overvoltage induced by the closing of the first switch will be nonuniformly added to the switches that are not yet closed. The switch with more overvoltage will close shortly after the closing of switch S_1. Once the second switch has been closed, the synchronization can be accomplished properly. Within the present system, the same magnetic cores were placed around the specific stages of the TLT, as shown in Fig. 4. Magnetic cores are not put around the cables of stages nos. 3, 6 and 8. The secondary mode impedances between two adjacent stages covered or not covered by magnetic cores are different. By means of this configuration, proper synchronization has been realized.

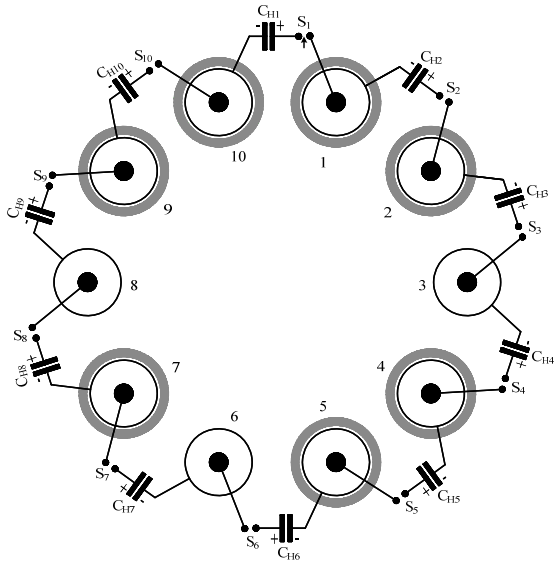

Fig. 4 Configuration of the magnetic cores around the coaxial cables of the TLT

The magnetic material used within the present system is metglass MP4510, and the length covered by magnetic material is 100 cm. With this material, the proper synchronization was obtained, and detailed information about its evaluation was reported in Ref. [16].

3.4 Compact Design

To obtain a fast rise-time, the structure must be as compact as possible. The ten switches S_1-S_{10}, the ten high-voltage capacitors C_{H1}-C_{H10}, and the input side of the TLT are integrated into one very compact structure, as shown in Figure 5. The ten switches are put into two arrays, with five switches per array. A compressed air flow is used to flush the spark gap switches for high-voltage and high repetition rate operations. This unit is able to hold a pressure up to 10 bar.

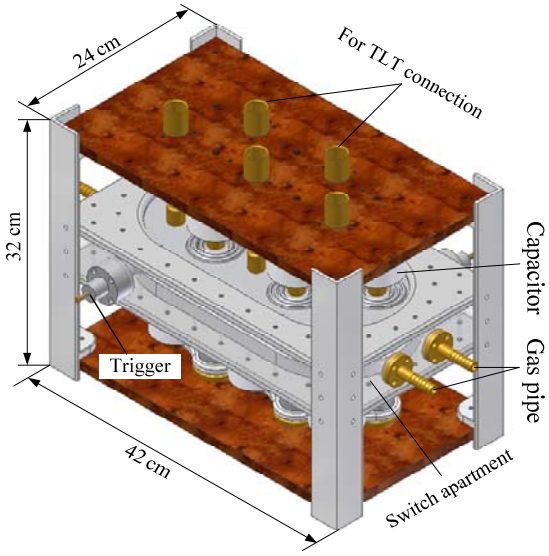

Fig. 5 Compact layout of components at the input side of the TLT

3.5 Output Characteristics

Fig. 6 shows the typical output voltage and current. For the ten-switch compartment, the input and output pressure were 3.4 bar and 2.4 bar respectively. The voltage on the high-voltage capacitors when the switches closed was 42.8 kV (switching voltage). The peak values of the output voltage and current are 48.4 kV and 6.46 kA respectively. The rise-times (10%-90%) of the output voltage and current are 11.0 ns and 12.2 ns respectively. In addition, it is seen that a small step with a duration of about 10.4 ns occurs within the rising part of the pulse (see magnified view in Fig. 6). This, in fact, implies that the ten spark gap switches are closed in sequence within about 10.4 ns.

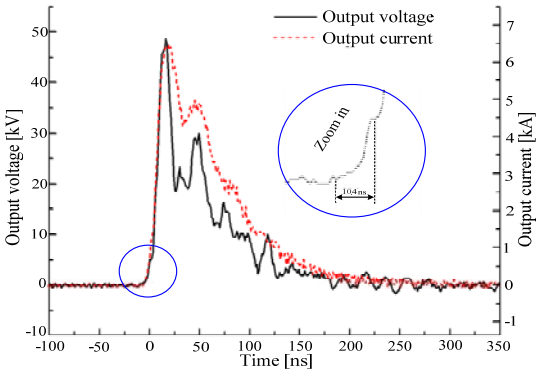

Fig. 6 Typical output voltage and current when the switching voltage was 42.8 kV

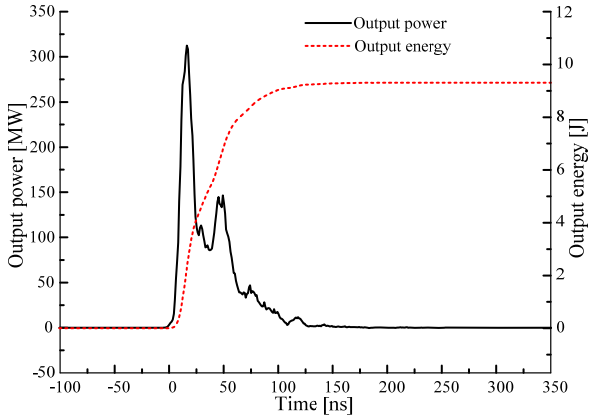

Fig. 7 The calculated output power and energy for the measurement shown in Fig. 6

Fig. 7 shows the output power and energy for the measurement shown in Fig. 6. The peak output power and the output energy are 312 MW and 9.31 J, respectively. The voltage on the high-voltage capacitors when the switches closed was 42.8 kV. Therefore, ideally (i.e. no energy loss and the TLT with a perfectly matched load), the value of the peak output power should be 366 MW. Due to the energy losses and the mismatching, the obtained peak power is 85% of the ideal value.

Besides the experiments described above, the testing was also carried out with the different switching voltages from 30 kV to 70 kV. The present system works well at different situations. When the setup was operated with a switching voltage of about 70 kV, the peak output power of 810 MW was obtained. And its peak output voltage, peak output current and output energy are 76.8 kV, 11.0 kA, and 24.1 J, respectively. In addition, the energy conversion efficiency of the ten-switch prototype was evaluated for different operation situations, and varies within the range between 93% and 98%.

4 CONCLUSIONS

A TLT based multiple-switch pulsed power technology is discussed. By interconnecting multiple spark gap switches via a TLT, multiple switches can be synchronized automatically, like in a Marx generator. In contrast to the Marx generator, the advantage is that pulsed power can be generated either at a high voltage or with a large current, or it can be used to drive independent loads simultaneously.

An efficient heavy-duty repetitive high voltage pulse generator with a fast rise-time and a short pulse width has been realized through use of this technology. The system has been operated properly at repetition rates up to 300 pps. Ten switches can be synchronized within about 10 ns. This system is able to produce pulses with a rise-time of about 11 ns and a width of about 55 ns. It has good reproducibility. The peak output power of 810 MW with a peak output current of about 11 kA was obtained. The energy conversion efficiency varies between 93% and 98%.

ACKNOWLEDGEMENTS

The presented work is finically supported by the Dutch IOP/EMVT program. Sincere thanks go to Mr. Ad van Iersel and Mr. R. T. W. J. van Hoppe for their helps on experiments.

REFERENCES

1. S. Levy, M. Nikolich, I. Alexeff, M. T. Buttram, and W. J. Sarieant. Commercial applications for modulators and pulse power technology. 20th Power Modulator Symposium, June 1992, 8-14.
2. M. Kristiansen. Pulsed power applications. 9th IEEE International Pulsed Power Conference, June 1993, 6-10.
3. K. Yan. Corona plasma generation. PhD diss., Eindhoven University of Technology, http://alexandria. tue.nl/ extra2/200142096.pdf, ISBN 90-386-1870-0, 2001.
4. K. Yan, E. J. M van Heesch, A. J. M. Pemen, P. A. H. J. Huijbrechts, and P. C. T. Van der Laan. A 10 kW high-voltage pulse generator for corona plasma generation. Rev. Sci. Instrum. Vol. 72, No. 5, May 2001, 2443-2447.
5. Yan, E. J. M van Heesch, A. J. M. Pemen, P. A. H. J. Huijbrechts, F. M. Van Gompel, H. Van Leuken, and Zdenek Matyas. A high-voltage pulse generator for corona plasma generation. IEEE Transactions on industrial applications, Vol. 38, No. 3, May/June 2002, 866-872.
6. E. J. M. van Heesch, K. Yan, and A. J. Pemen. Heavy-duty high-repetition-rate generators. IEEE transactions on plasma science, Vol. 30, No. 5, October 2002, 1627-1631.
7. K. Yan, E. J. M. van Heesch, P. A. A. F. Wouters, A. J. M. Pemen, and S. A. Nair. Transmission line transformers for up to 100 kW pulsed power generation. 25th international Power Modulator Symposium and High-Voltage Workshop, 30 June-3 July 2002, 420-423.
8. J. C. Dickens, T. G. Engel, and M. Kristiansen. Electrode performance of a three electrode triggered high energy spark gap switch. 9th IEEE International Pulsed Power Conference, 21-23 June, 1993, 471-474.
9. L. Donaldson, T. G. Engel, and M. Kristiansen. State-of-the-art insulator and electrode materials for use in high current high energy switching. IEEE Transactions on Magnetics, Vol. 25, Issue 1, 138-141.
10. F. M. Lehr, and M. Kristiansen. Electrode erosion from high current moving arcs. IEEE Transactions on Plasma Science, Vol. 17, No. 5, October 1989.
11. K. Yan, H. W. M. Smulders, P. A. A. F. Wouters, S. Kapora, S. A. Nair, E. J. M. van Heesch, P. C. T. van der Laan, and A. J. M. Pemen. A novel circuit topology for pulsed power generation. Journal of Electrostatics, Volume 58, Issues 3-4, June 2003, 221-228.
12. Z. Liu, K. Yan, A. J. M. Pemen, G. J. J. Winands, and E. J. M. Van Heesch. Synchronization of multiple spark-gap switches by a transmission line transformer. Review of Scientific Instruments, Vol. 76, Issue 11, (113507) 2005.
13. Z. Liu, K. Yan, G. J. J. Winands, A. J. M. Pemen, E. J. M. Van Heesch, and D. B. Pawelek. 2006. Multiple-gap spark-gap. Review of Scientific Instruments, Vol. 77, Issue 07, (073501) 2006.et
14. Z. Liu, K. Yan, G. J. J. Winands, E. J. M. Van Heesch, and A. J. M. Pemen. Novel multiple-switch Blumlein generator. Review of Scientific Instruments, Vol. 77, Issue 03, (033502) 2006.
15. K. Yan, E. J. M. van Heesch, S. A. Nair, and A. J. M. Pemen. A triggered spark-gap switch for high-repetition rate high-voltage pulse generation. Journal of Electro-statics, 57 (2003), 29-33.
16. Z. Liu. Multiple-switch pulsed power generation based on a transmission line transformer. PhD diss., Eindhoven University of Technology, available at: http://alexandria. tue.nl/extra2/200712432.pdf, 2008, ISBN 978-90-386-1764-0.